Human Molecular Genetics, 2011, Vol. 20, No. 15 **3079–3092**
doi:10.1093/hmg/ddr211
Advance Access published on May 10, 2011

Altered zinc transport disrupts mitochondrial protein processing/import in fragile X-associated tremor/ataxia syndrome

Eleonora Napoli[1], Catherine Ross-Inta[1], Sarah Wong[1], Alicja Omanska-Klusek[1], Cedrick Barrow[1], Christine Iwahashi[2], Dolores Garcia-Arocena[2], Danielle Sakaguchi[1], Elizabeth Berry-Kravis[5], Randi Hagerman[3,4], Paul J. Hagerman[2,4] and Cecilia Giulivi[1,*]

[1]Department of Molecular Biosciences, School of Veterinary Medicine, [2]Department of Biochemistry and Molecular Medicine, [3]Department of Pediatrics and [4]MIND Institute, School of Medicine, University of California Davis, Davis, CA 95616, USA and [5]Department of Pediatrics, Neurological Sciences, and Biochemistry, Rush University Medical Center, Chicago, IL 60612, USA

Received January 14, 2011; Revised and Accepted May 6, 2011

Fragile X-associated tremor/ataxia syndrome (FXTAS) is a late-onset neurodegenerative disorder that affects individuals who are carriers of small CGG premutation expansions in the fragile X mental retardation 1 (*FMR1*) gene. Mitochondrial dysfunction was observed as an incipient pathological process occurring in individuals who do not display overt features of FXTAS (1). Fibroblasts from premutation carriers had lower oxidative phosphorylation capacity (35% of controls) and Complex IV activity (45%), and higher precursor-to-mature ratios (P:M) of nDNA-encoded mitochondrial proteins (3.1-fold). However, fibroblasts from carriers with FXTAS symptoms presented higher *FMR1* mRNA expression (3-fold) and lower Complex V (38%) and aconitase activities (43%). Higher P:M of ATPase β-subunit (ATPB) and frataxin were also observed in cortex from patients that died with FXTAS symptoms. Biochemical findings observed in FXTAS cells (lower mature frataxin, lower Complex IV and aconitase activities) along with common phenotypic traits shared by Friedreich's ataxia and FXTAS carriers (e.g. gait ataxia, loss of coordination) are consistent with a defective iron homeostasis in both diseases. Higher P:M, and lower ZnT6 and mature frataxin protein expression suggested defective zinc and iron metabolism arising from altered ZnT protein expression, which in turn impairs the activity of mitochondrial Zn-dependent proteases, critical for the import and processing of cytosolic precursors, such as frataxin. In support of this hypothesis, Zn-treated fibroblasts showed a significant recovery of ATPB P:M, ATPase activity and doubling time, whereas Zn and desferrioxamine extended these recoveries and rescued Complex IV activity.

INTRODUCTION

Fragile X-associated tremor/ataxia syndrome (FXTAS) is a late-onset neurodegenerative disorder (2–4) that affects individuals who are carriers of premutation expansions (55–200 CGG repeats) in the 5′untranslated region (5′UTR) of the fragile X mental retardation 1 (*FMR1*; OMIM *309550) gene. FXTAS typically affects carriers (males > females) over 50 years of age, with core features of action tremor and gait ataxia, but also (more variably) parkinsonism, executive dysfunction, cognitive decline, neuropathy and autonomic dysfunction. The core neuropathologic feature of FXTAS is the presence of *FMR1* mRNA–containing inclusions in the nuclei of neurons and astrocytes of affected individuals (5–7), consistent with the 'RNA toxicity' model of pathogenesis (3). Larger expansions (>200 CGG repeats; full mutation) generally result in transcriptional silencing and absence of the *FMR1* mRNA and protein product (8–11),

*To whom correspondence should be addressed at: Department of Molecular Biosciences, University of California Davis, 1120 Haring Hall, One Shields Avenue, Davis, CA 95616, USA. Tel: +1 5307548603; Fax: +1 5307524698; Email: cgiulivi@ucdavis.edu

leading to fragile X syndrome, the most common heritable form of cognitive impairment and leading known form of autism. Individuals with the full mutation are not at-risk for FXTAS or the fragile X-associated primary ovarian insufficiency, as in these cases the toxic *FMR1* mRNA is absent or present at low levels.

Given that several symptoms of FXTAS, including gait ataxia, white matter disease, dysautonomia, peripheral neuropathy, weakness/exercise intolerance and neuropsychiatric involvement, overlap those of mitochondrial respiratory enzyme chain enzyme deficiencies, we recently investigated and identified mitochondrial dysfunction (MD) in both cultured dermal fibroblasts and brain samples from individuals with the **p**remutation with FXTAS **s**ymptoms (PS) and without FXTAS symptoms (**p**remutation **a**symptomatic or PA) with CGG repeat length at the low end of the premutation range (1). Our study resulted in several important conclusions: (i) decreased nicotinamide adenine dinucleotide- and flavin adenine dinucleotide-linked oxygen uptake rates and uncoupling between electron transport and synthesis of ATP; (ii) a lower expression of mitochondrial proteins preceded clinical involvement, even in younger carriers with smaller CGG repeat lengths; (iii) the CGG repeat size required for altered mitochondrial protein expression was also lower than the lower bound of CGG repeat size associated with intranuclear inclusions observed to date in individuals who died with FXTAS, suggesting that MD is an incipient pathological process occurring in individuals who do not display overt features of FXTAS; (iv) for a given CGG repeat, MD preceded the increase in oxidative/nitrative stress damage indicating that the latter is a late event (1).

Thus, the goals of the present study were to elucidate the mechanisms underlying the MD observed in premutation carriers of comparable age and CGG repeat expansions, and if this mechanism would show differences between premutation carriers with (PS) and without (PA) symptoms of FXTAS that would explain the clinical phenotype.

RESULTS

Clinical characteristics of individuals with FXTAS with and without symptoms

The subjects included in this study were all males referred to the Chicago or UC Davis clinics either because they presented with FXTAS symptoms, including tremor and/or ataxia, or were either premutation carriers ascertained through families with a fragile X syndrome proband, or controls in a similar age group range. Individuals contributing skin biopsies were participants in a multicenter study to characterize neurological findings in premutation carriers. Primary cultured skin fibroblasts from the skin biopsies were obtained from 14 male premutation carriers: 8 with FXTAS symptoms (identified in Tables as PS) and 6 without FXTAS symptoms (or asymptomatic, identified in Tables as PA) and 7 controls (Table 1 and Supplementary Material, Table S1). There was no statistical difference in age between the control group (64 ± 2 years old) and the premutation carriers (PA: 71 ± 2 and PS: 68 ± 3 years old; Table 1). For the fibroblast samples, there was a significant difference between CGG repeat numbers between PS and PA (96 ± 7 and 69 ± 2, mean $\pm$ SEM, respectively; $P = 5 \times 10^{-3}$; Table 1), and both groups were significantly different from controls (CGG repeat for controls 27 ± 2 with $P = 2 \times 10^{-8}$ to PA and $P = 4 \times 10^{-7}$ to PS; Table 1). On average, there was a gap of 9 ± 2 years between the onset of FXTAS symptoms and the time of the skin biopsy.

Table 1. Clinical characteristics of the individuals from which the cultured primary dermal fibroblasts were obtained and utilized in this study

Group (n)	Age (years)	CGG repeats	Stage	*FMR1* transcript level (% of control)
Control ($n = 7$)	64 ± 2	27 ± 2	0	100
PA ($n = 6$)	71 ± 2	69 ± 2	0	97 ± 3
P-value to controls	0.042	2×10^{-8}		–
PS ($n = 8$)	68 ± 3	96 ± 7	3.8 ± 0.2	350 ± 50
P-value to controls		4×10^{-7}		0.001
P-value to PA		5×10^{-3}		0.002

Stages were defined as indicated previously (1). The CGG repeats differ from those previously published (1) because these were determined from the gDNA from dermal fibroblast grown in culture (not from original biopsy) under the conditions indicated under Materials and Methods. All individuals were male and further clinical data of these individuals were provided under Supplementary Material, Table S1. The level of *FMR1* transcript (normalized to beta-2-microglobulin) was obtained from primary dermal fibroblasts from each group of individuals as described under Materials and Methods.

It could be argued that primary dermal fibroblasts do not constitute an appropriate model system to address mitochondrial function in FXTAS because the level of *FMR1* transcript overexpression in fibroblasts may not necessarily mimic that in neurons. The *FMR1* transcript levels in PA and PS cells were $97 \pm 3\%$ ($P = 0.97$) and $350 \pm 50\%$ ($P = 0.001$), respectively, of control values (Table 1). These results indicated that primary fibroblasts in culture from PS do over-express *FMR1* transcript and that the levels of the expanded CGG-repeat *FMR1* mRNA are similar to those observed in FXTAS neurons (from 2- to 8-fold in premutation carriers; 12–14). Moreover, there is increasing evidence that the underlying pathogenesis of FXTAS also results in additional systemic [non-central nervous system (CNS)-related] dysregulation, including the formation of intranuclear inclusions, in cells of the peripheral nervous system, and in diverse organ tissues (15,16; C.G. and P.J.H., unpublished data).

Lower oxidative phosphorylation capacity in cultured fibroblasts from premutation carriers is linked to lower Complex IV and/or V activities

The rates of oxygen uptake by primary cultured fibroblasts obtained from PA, PS and controls were obtained in a glucose-containing media supplemented with oligomycin (State 4 or non-phosphorylating conditions) and subsequently with FCCP, an uncoupler (State 3u). In PA fibroblasts, no statistical difference with respect to controls was observed in the oxygen uptake in State 4 (Table 2); however, PS cells exhibited a 2.6-fold increase ($P = 0.05$; Table 2). The rates of oxygen

Table 2. Rates of oxygen uptake in State 3u and State 4, RCRu and glucose consumed in OXPHOS by primary PA, PS and control fibroblasts

Group	Oxygen uptake rate (nmol $O_2 \times (\text{min} \times 10^6 \text{ cells})^{-1}$)			RCRu	Glucose consumed in OXPHOS (nmol $\times$ (min $\times$ 10^6 cells)$^{-1}$)
	Basal	State 4	State 3u		
Control ($n = 5$)	4.7 ± 0.6	1.0 ± 0.2	9 ± 1	11 ± 2	0.54 ± 0.09
PA ($n = 4$)	2.8 ± 0.6	1.4 ± 0.7	4.0 ± 0.8	5 ± 1	0.22 ± 0.03
P-value to controls	–	–	0.03	–	0.02
PS ($n = 6$)	5 ± 1	2.6 ± 0.6	5.1 ± 0.9	3.1 ± 0.9	0.16 ± 0.07
P-value to controls	–	0.05	0.05	0.05	0.02
P-value to PA	–	–	–	–	–

Oxygen uptake rates were taken at 22°C with cells suspended in high glucose DMEM buffer (25 mM in glucose; basal) supplemented with 5 μg/ml oligomycin (State 4), subsequently supplemented with 5 nM FCCP (State 3u). RCRu was calculated by dividing the State 3u rates by the State 4 rate. Glucose consumption was obtained as the rate of oxygen consumption sensitive to oligomycin divided by 6 (6 oxygen consumed per glucose). The *P*-values were obtained from unpaired two-tailed *t*-test. Other experimental details were described under Materials and Methods.

uptake of PA or PS cells in State 3u were half of control values ($P = 0.03$ and 0.05; Table 2). The respiratory control ratio (RCR) evaluates the coupling between electron transfer and oxidative phosphorylation (OXPHOS). Fully uncoupled mitochondria have RCR values of 1 (17,18). Control cells were fully coupled with a respiratory control ratio in the presence of uncoupler (RCRu) of 11 ± 2, whereas PA cells had lower RCRu, but not significantly different from controls (Table 2). The RCRu of PS cells was 3.1 ± 0.9 indicating that the mitochondria were substantially uncoupled (Table 2). The higher uncoupling (lower RCRu) observed in PS was the result of both an increase in State 4 oxygen uptake and a decrease in State 3u (Table 2). Of note, the higher uncoupling of electron transport with ATP synthesis was statistically significant only in cells from PS individuals, suggesting a segregation of the severity of MD with the presence of FXTAS symptoms.

To evaluate whether the decreased mitochondrial function had an impact in the glucose consumed by the cells via OXPHOS, the rate of oligomycin-sensitive oxygen uptake in a glucose-supplemented media was evaluated in control, PS and PA cells. In PA cells, the rate of glucose uptake in OXPHOS was 41% of controls ($P = 0.02$), whereas in PS was 30% of controls ($P = 0.02$). These results indicated that premutation cells had a lower rate of glucose oxidation via OXPHOS, suggesting that a higher proportion of their ATP is derived from anaerobic glycolysis especially in PS cells, consistent with the presence of symptoms in these individuals.

No significant changes in either mtDNA copy number or mitochondrial mass was found between cells from premutation carriers and controls indicating that the lower oxygen uptake rate in State 3u and glucose consumption via OXPHOS found in premutation cells could not be explained by lower mitochondrial number (estimated by means of mtDNA content or citrate synthase activity; Supplementary Material, Table S2). In fact, the mtDNA copy number in PS cells was 1.34-fold of controls ($P = 0.008$), suggesting a cellular response to overcome oxidative stress as described in other biological models (19–23). To evaluate increased oxidative stress and considering that mitochondria are the main intracellular source of reactive oxygen species (ROS; 24), the rate of hydrogen peroxide production was evaluated in control and PS fibroblasts using succinate (in the presence of rotenone and antimycin) and NADH (in the presence of rotenone). This experimental design allowed testing for ROS production by Complex III and Complex I, respectively. Our results indicated that the ROS production was significantly enhanced [2.4-fold; controls $= 0.08 \pm 0.02$ and PS: 0.19 ± 0.05 nmol $H_2O_2 \times (\text{min} \times 10^7 \text{ cells})^{-1}$; $P < 0.05$] in PS cells at the level of Complex I, whereas no significant difference was obtained at Complex III.

Table 3. Activities of mitochondrial electron transport chain Complexes in control, PA and PS primary fibroblasts

Group	Complex activities normalized to citrate synthase (mean $\pm$ SEM)				
	Complex I		Complexes II–III	Complex IV	Complex V
	NQR	NFR	SCCR	CCO	ATPase
Controls ($n = 5$)	8 ± 2	6.1 ± 0.7	0.19 ± 0.03	1.8 ± 0.3	2.1 ± 0.5
PA ($n = 4$)	8 ± 2	7 ± 2	0.27 ± 0.07	0.6 ± 0.1	1.5 ± 0.2
P-value to controls	–	–	–	0.01	–
PS ($n = 6$)	6 ± 1	6 ± 2	0.13 ± 0.01	1.0 ± 0.2	0.8 ± 0.2
P-value to controls	–	–	–	0.05	0.02
P-value to PA	–	–	–	–	0.02

Individual values represent the mean of duplicate or triplicate experiments. The *P*-values were obtained from Student *t*-test. Other experimental details were described under Materials and Methods.
NFR, NADH-ferricyanide oxidoreductase; NQR, NADH-decylubiquinone oxidoreductase.

To determine whether the lower OXPHOS capacity accompanied by a higher ROS rate observed in cells from premutation carriers was the result of a defect at any of the electron transport chain Complexes, the activities of each were tested (Table 3). In premutation cells, the activity of cytochrome *c* oxidase (Complex IV) was 33% (PA) and 56% (PS) of control values ($P = 0.01$ and 0.05, respectively; Table 3). In addition, in PS cells only, the activity of ATPase (Complex V) was 38% of the controls ($P = 0.02$; Table 3) and significantly different from PA (53% with $P = 0.02$). The lower Complex IV activity in cells from premutation carriers was consistent with the lower rates of State

3u oxygen uptake and glucose consumption via OXPHOS observed above (Table 2). More importantly, the lower ATPase activity in PS cells segregated with the presence of FXTAS symptoms.

No other mean Complex activity in premutation cells resulted in a statistical significant difference from controls. However, three out of five PS samples showed lower Complex I (below 95% CI) and two out of four had lower Complex II–III activities, whereas in PA samples only one had low Complex I activity and none showed low succinate cytochrome *c* reductase (SCCR) activity, suggesting that Complexes other than IV and V were also affected in premutation carriers with symptoms than in those without.

Defective import/processing of mitochondrial precursors in FXTAS fibroblasts

The lower Complex IV (PS and PA) and V (PS only) activities observed in premutation cells could result from one or both of the following processes: (i) decreased steady-state levels of certain mitochondrial subunits resulting from decreased synthesis, increased proteolysis or a combination of both processes; (ii) a defective processing, assembly and/or import of nuclear-encoded proteins resulting in lower mitochondrial activities.

To ascertain if the lower Complex activities were the result of lower protein expression, western blots were performed to evaluate the levels of several subunits from Complexes I, IV and V (Supplementary Material, Table S3). For all 10 proteins tested, 6 in PA and 7 in PS were significantly lower compared with controls (60 ± 7 and 57 ± 5% of controls for PA and PS, respectively). However, the lack of correlation between Complex activities (Table 3) and subunit protein expression in premutation cells (Supplementary Material, Table S3) indicated that the steady-state levels of the individual Complex subunits did not translate (in most of the cases) into activity loss. The lack of a more consistent correlation seemed to reflect a defective processing of precursor proteins, import or assembly of Complexes resulting in higher instability of the assembled Complexes, rather than an increased degradation or decreased synthesis of the individual subunits.

Considering that the rates of the import/processing of mitochondrial precursor proteins (or preproteins) are generally one order of magnitude faster than their rates of degradation in the cytosol (25,26), a defect at the processing and/or import levels may result in the accumulation of precursor proteins in the cytosol. To this end, we evaluated the mature and precursor protein expression of ATPB (subunit of Complex V), cytochrome *c* oxidase (CCO4, subunit IV of Complex IV) and NADH dehydrogenase (ubiquinone) Fe-S protein 4, 18 kDa (NDUFS4, subunit of Complex I) in control and premutation cells (Table 4). Our experimental conditions do not allow discerning MW differences of <5 kDa between precursor and mature mitochondrial proteins, thus from the 10 proteins tested (Supplementary Material, Table S3), only NDUFS4, CCO4 and ATPB fulfilled this requirement.

The ATPB precursor-to-mature ratio (P:M) was significantly increased in PA (4.6-fold of controls; $P = 0.03$) and PS (2.5-fold of controls; $P = 0.01$; Table 4 and Fig. 1A). Consistent with the results obtained on ATPB, an altered P:M was also observed for CCO4 and NDUFS4 in premutation cells. The P:M of CCO4 (Fig. 1A and Table 4) and NDUFS4 (Table 4) was significantly increased in both PA (CCO4: 3.5-fold of controls; $P = 0.04$; NDUFS4: 2-fold of controls; $P = 0.024$) and PS (CCO4: 3.8-folds; $P = 0.035$; NDUFS4: 2.3-fold of controls; $P = 0.014$) (Table 4). The expression levels of CCO2, an mtDNA-encoded subunit, were also examined in dermal fibroblasts from controls and PS carriers. As expected for a defect in the import/processing step, no differences were found in the expression levels of this protein between controls and PS (normalized to actin; controls = 0.35 ± 0.06; PS = 0.34 ± 0.1; Supplementary Material, Fig. S1 and Table S3).

In PS cells, the higher P:M, the lower mature ATPB content (42 ± 14% of controls; $P = 0.02$) and the lower ATPase activity (38 ± 10% of controls; $P = 0.02$) suggested that the processing of ATPB (as well as other proteins synthesized in the cytosol, i.e. NDUFS4 and CCO4) was limiting, resulting in dysfunctional mitochondria. Although similar conclusions could be reached with PA cells, the relatively lower increase in the P:M in conjunction with a relatively higher content of mature ATPB (62 ± 13% of controls; $P = 0.04$) compared with PS cells could explain the lack of ATPase activity decline in PA cells.

It could be inferred that changes in P:M may be attributed to the age difference between groups since premutation patients were older than controls (77 ± 3 and 58 ± 4; $P = 0.002$; Table 5); however, P:M as well as the mature and precursor ATPB levels decreased significantly with the CGG repeat expansion [as reported before (1)] but not with age in both controls and PS (Supplementary Material, Fig. S2).

Table 4. ATPB, NDUFS4 and CCO4 precursor-to-mature ratios in skin fibroblasts from premutation carriers

	P:M (mean ± SEM in % of controls)		
	NDUFS4	CCO4	ATPB
PA ($n = 5$)	198 ± 29	348 ± 90	464 ± 136
P-value to controls	0.02	0.04	0.03
PS ($n = 5$)	233 ± 44	376 ± 81	248 ± 50
P-value to controls	0.01	0.03	0.01
P-value to PA	–	–	–

The ratios of intensities at precursor and mature MW bands were evaluated in total cell lysates (see Figure 1 for an example of P and M bands). The P:M for control cells was 0.27 ± 0.05 for NDUFS4, 0.66 ± 0.06 for CCO4 and 0.20 ± 0.04 for ATPB.

Defective import/processing of ATPB and frataxin in brains from patients that died with FXTAS symptoms

To confirm the results obtained with fibroblasts, the P:M levels of ATPB were analyzed in brain samples from patients that died with FXTAS symptoms (clinical characteristics of patients in Table 5 and Supplementary Material, Table S4). The abnormal ATPB P:M observed in premutation carriers was also detected in frontal cortex samples (Fig. 1B), mitigating concerns that the foregoing observations may reflect either an exclusive property of dermal fibroblasts or as an artifact of culture conditions.

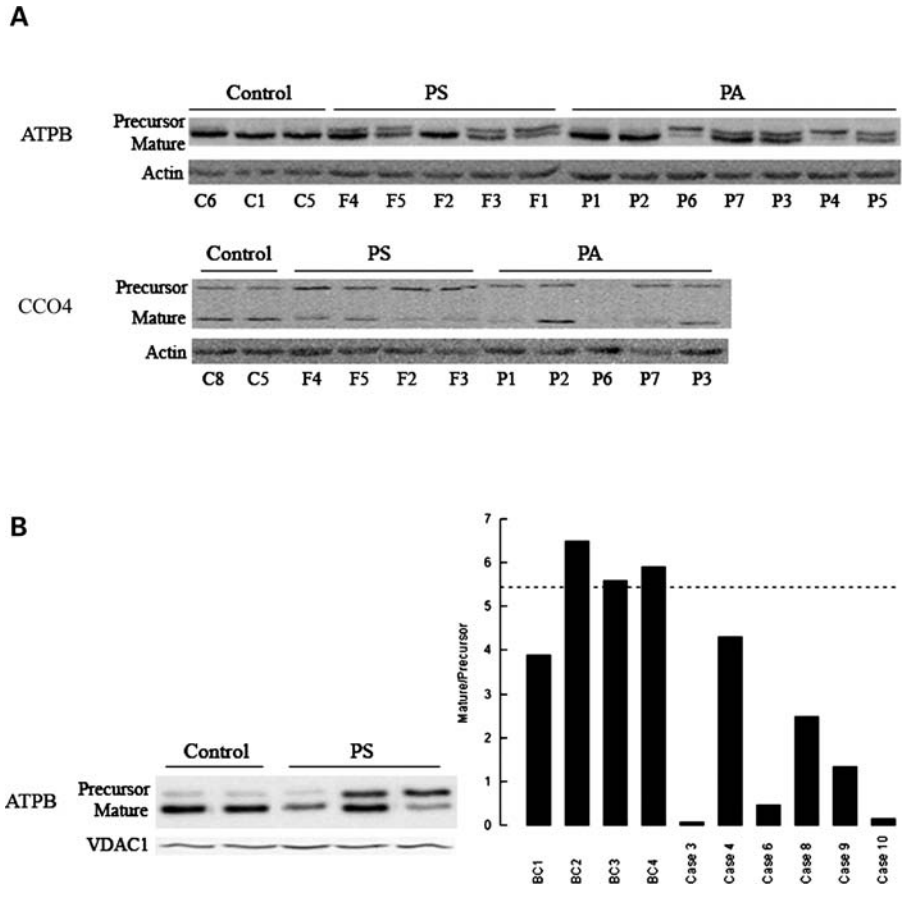

Figure 1. Mitochondrial protein expression in cultured primary dermal fibroblasts and frontal brain cortex samples from premutation patients. (**A**) Western blots of fibroblasts from control, PS and PA carriers. Representative western blot of the fibroblast panel probed for ATPB and CCO4 (precursor and mature proteins). Actin was used as a loading control. Samples were identified by following the nomenclature indicated under Supplementary Material, Table S1 with the exception of P7, which was described before (1). (**B**) Representative western blot of some of the brain samples indicated under Supplementary Material, Table S4. The densitometry for all the cortex samples is also shown. The samples were probed for ATPB and normalized by VDAC1 (loading control). Data were expressed as Arbitrary Densitometry Units and reported as P:M.

Table 5. Clinical characteristics of the individuals from which the brain samples were utilized in this study

Group (n)	Age (years)	CGG repeats
Control ($n = 4$)	58 ± 4	24 ± 3
PS ($n = 6$)	77 ± 3	83 ± 5
P-value	0.002	2×10^{-5}

Clinical and molecular characteristics of the panel of postmortem brain samples (frontal cortex) used in this study correspond in case number to those presented previously (1) and further described under Supplementary Material, Table S4. All individuals were male and the brain samples were kept at −80°C until the protein samples were obtained.

Frataxin, a protein involved in mitochondrial iron homeostasis, is a nuclear-encoded mitochondrial protein whose precursor (P, MW = 23.1 kDa) is converted to the mature (M, MW = 14.3 kDa) form through a two-step proteolytic processing via formation of an intermediate (I, MW = 18.8 kDa) polypeptide chain (27,28). To test whether the import/processing of this protein was also impaired in FXTAS brain samples, western blots were performed to evaluate the levels of frataxin P, I and M. As observed for ATPB, NDUFS4 and CCO4 in PS fibroblasts, and for ATPB in cortex samples from PS, significantly lower mature frataxin levels (normalized by actin: 2.8-fold; $P = 0.004$) and significantly higher P:M and I:M (6.3-fold; $P = 0.04$ and 15-fold; $P = 0.008$) were observed in brain samples from FXTAS patients compared with controls (Fig. 2), further confirming a generalized defect in the import/processing machinery of mitochondrially targeted proteins.

Impaired AFG3l2 and mitochondrial processing peptidase activities are not related to lower protein or transcript expression

Mice deficient in ATPase family gene 3-like 2 (AFG3l2) and its partner protein, paraplegin (SPG7), show tremor and ataxia as well as mitochondrial abnormalities (29). In yeast, AFG3 and RCA1 constitute the *m*-AAA protease complex that mediates the degradation of non-assembled mitochondrial inner membrane proteins. This complex is necessary for the assembly of mitochondrial respiratory chain and ATPase Complexes and has an important function in both post-translational

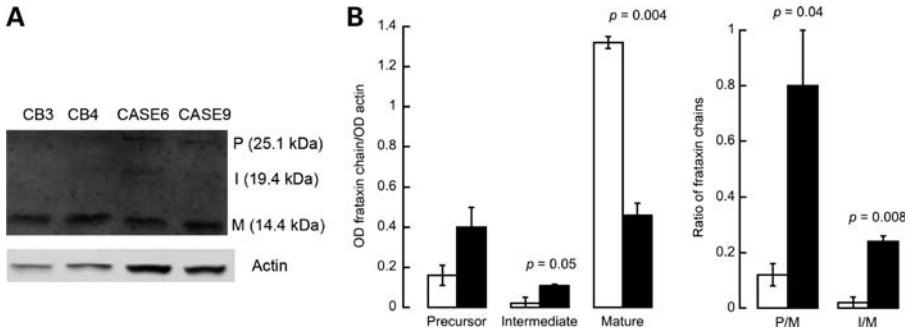

Figure 2. Frataxin protein expression in frontal brain cortex samples from premutation patients. (**A**) Western blots of some of the brain samples indicated under Supplementary Material, Table S4. Samples were probed for frataxin and normalized by actin (loading control). (**B**) Densitometry of frataxin precursor (P), intermediate (I) and mature (M) polypeptides was expressed as Arbitrary Densitometry Units (ADU) and reported as frataxin expression normalized by actin or as precursor-to-mature (P:M) and intermediate-to-mature (I:M) frataxin. Black bars, premutation carriers. White bars, controls.

assembly and turnover of mistranslated or misfolded polypeptides. Thus, the transcript and protein expression of several mitochondrial proteases [including AFG3l2, SPG7 and mitochondrial processing peptidase subunits A and B, or mitochondrial processing peptidase subunit alpha (MPPA) and MPPB, which specifically remove the *N*-terminal transit peptides from precursors imported into the mitochondrion, including frataxin (30,31) and ATPB (28,32,33)] were evaluated by quantitative, real-time polymerase chain reaction (qPCR) and western blotting in premutation cells. Protein expression of AFG3l2 and MPPB in PA was not significantly different from controls (Supplementary Material, Fig. S3); however, in PS, AFG3l2 and MPPB protein levels were higher than control levels ($154 \pm 16\%$ of controls with $P = 7 \times 10^{-3}$ and $133 \pm 11\%$ of controls with $P = 0.03$; Supplementary Material, Fig. S3). Transcript levels of AFG3l2, SPG7, MPPA and MPPB in PS were all significantly higher than controls (average 2.3-fold of controls; Supplementary Material, Fig. S3), whereas in PA only SPG7 and MPPB were higher than controls (1.94-fold of controls; Supplementary Material, Fig. S3). Thus, the lower activities of Complexes IV (PS and PA) and V (PS only) observed in premutation carriers could not be explained by changes in the protein levels of these proteases, when in fact they were at levels comparable to (PA) or higher (MPPB and AFG3l2 in PS) than controls (Supplementary Material, Fig. S3B). The higher transcript levels of AFG3l2, SPG7, MPPA and MPPB observed in PS seemed to be a compensatory cellular response to overcome a lower processing of nDNA-encoded mitochondrial proteins, excluding a dysfunctional transcription and/or translation, at least for these proteases, in premutation cells. However, the lower activity of these proteases—evidenced by the accumulation of mitochondrial precursors—pointed at lower protease activities not accompanied by the higher protein and transcript expression.

Zinc supplementation and iron chelation decreases the precursor-to-mature ratio and the doubling time while rescuing Complex V and IV activities in PS cells

Considering that AFG3l2, SPG7 and MPP are zinc-dependent proteases (34), we tested the hypothesis that zinc was limiting in PS cells, leading to a lower content of active holoproteases. Furthermore, given the abnormal frataxin levels found in cortex samples of FXTAS patients, we tested the hypothesis that deficits in frataxin result in iron accumulation in PS cells, leading to the observed loss in aconitase and Complex IV activity, enzymatic activities known to be defective in frataxin-deficient cells (35).

Table 6. Effect of zinc and DFO additions to dermal fibroblasts from PS patients on doubling time, ATPB precursor-to-mature ratios and Complex V and IV activities

Outcome	Percentage of vehicle-treated PS		
	Zinc	DFO	DFO + zinc
Doubling time	49 ± 5	49 ± 4	37 ± 8
P-value	0.04	0.04	0.03
P:M	87 ± 2	77 ± 4	71 ± 1
P-value	0.05	0.03	0.01
Complex IV activity	105 ± 12	132 ± 8	131 ± 7
P-value	–	0.006	0.01
Complex V activity	148 ± 15	114 ± 15	178 ± 25
P-value	0.01	–	0.005

Controls and PS were treated with vehicle (0.01% DMSO), zinc (20 μM $ZnCl_2$), DFO (40 nM DFO) and DFO + zinc (40 nM DFO and 20 μM $ZnCl_2$) for 48 h. At the end of the incubation time, cells were harvested and counted, and the activities of Complexes V and IV were evaluated along with western blots probing for the P:M of ATPB. The activities of Complexes V and IV were normalized to citrate synthase activity. For those numbers that were significantly different from their respective controls (i.e. PS treated with vehicle only), the *P*-values are shown. Other experimental details were described under Materials and Methods.

To this end, control and PS cell lines were subjected to four different conditions: (i) vehicle only (0.01% DMSO); (ii) supplementation with $ZnCl_2$; (iii) desferrioxamine mesylate (DFO), a specific chelator of labile ferric ion ($K_{d(Fe)} = 10^{-31}$ M; $K_{d(Zn)} = 10^{-11}$ M; 36), and (iv) DFO plus $ZnCl_2$. After 48 h, the doubling time, P:M and Complex IV and V activities were evaluated in fibroblasts (Table 6 and Supplementary Material, Fig. S4).

The concentration of $ZnCl_2$ tested in these experiments (20 μM) was in the range of those used for the kinetics of zinc uptake by human fibroblasts (5–40 μM; 37–39) and similar to the plasma zinc concentration (15 μM; 40). Supplementation of the cells with 20 μM $ZnCl_2$ resulted in ~1–2 fmol zinc/cell [estimated from the rates and V_{max} of zinc uptake from ref. (37)]. The concentration of the DFO

Table 7. Gene and protein expression levels of ZnT4 and ZnT6 in dermal fibroblasts from controls, PS and PA patients

	Gene and protein expression for ZnT (% of control values)			
	Gene expression		Protein expression	
	ZnT4	ZnT6	ZnT4	ZnT6
PA fibroblasts ($n = 4$)	85 ± 10	49 ± 27	82 ± 18	51 ± 16
PS fibroblasts ($n = 3$)	68 ± 28	40 ± 31	71 ± 14	14 ± 7 $P = 6 \times 10^{-3}$

For gene expression, PCR was performed on cDNA obtained from RNA extracted from controls, PA and PS as described under Materials and Methods. Evaluation of ZnT family members expression in human fibroblasts followed essentially that described by Falcon-Perez and Dell'Angelica (110) with the modifications indicated in the Materials and Methods section. The PCR products were visually detected by staining the gels with ethidium bromide. The protein expression was performed by western blots and probing for ZnT4 and ZnT6 (normalized to tubulin and actin, respectively) as described under Materials and Methods. Gene expression values for control cells were $125\,387 \pm 29\,886$ ZnT4, $118\,203 \pm 53\,521$ ZnT6; the protein expression values for control cells were 19.4 ± 13.6 ZnT4, 9.17 ± 2.8 ZnT6. Images of PCR products were reported in Supplementary Material, Figure S5. All values in the table were expressed as percentage of mean control values ($n = 3$). The *P*-values were obtained compared with control values.

was calculated to sequester most of the labile heavy metals (molar ratio of metal to chelator = 1/1), without resulting in significant intracellular metal mobilization, which would have obscured the outcome or have been toxic (DFO concentrations ≥ 10 μM resulted in cell detachment within 1 h of incubation in controls and PS cells).

All treatments significantly decreased the doubling time of PS cells compared with vehicle-treated PS (Table 6 and Supplementary Material, Fig. S4A), suggesting that zinc supplementation and/or iron chelation improved cell proliferation. Addition of zinc to PS cells significantly decreased the P:M (by 13%; $P = 0.05$; Table 6 and Supplementary Material, Fig. S4B) and increased Complex V activity (1.5-fold; $P = 0.01$; Table 6 and Supplementary Material, Fig. S4D) compared with vehicle-treated PS. Addition of DFO decreased the P:M (by 23%; $P = 0.03$) and increased the specific activity of Complex IV (on average by 1.3-fold; $P = 0.006$) compared with vehicle-treated PS cells (Table 6 and Supplementary Material, Fig. S4C). Addition of both zinc and DFO decreased the P:M (by 29%; $P = 0.01$) and increased both Complex IV (1.3-fold, $P = 0.01$) and Complex V (1.8-fold; $P = 0.005$) activities. Of note, the addition of both zinc and DFO to PS cells showed an improvement that, for some of the outcomes (namely doubling time, ATPase activity and Complex IV activity), was more significant than that obtained by individual treatments. Doubling time of cells treated with Zn + DFO decreased an additional 32% compared to the treatment with Zn and an additional 38% compared to the treatment with DFO ($P = 0.04$). ATPase activity of cells treated with DFO + Zn was 1.2-fold of that with Zn only and 1.6-fold of that obtained with DFO only ($P = 0.05$). Complex IV activity in the presence of Zn and DFO was 1.3-fold of that obtained with Zn only ($P = 0.05$).

To evaluate the effect of the various treatments on PS cells compared with vehicle-treated controls, comparisons for each outcome were made between these two experimental groups (Supplementary Material, Fig. S4). For all treatments, the doubling time (Supplementary Material, Fig. S4A) and Complex IV activity (Supplementary Material, Fig. S4C) of PS cells resulted in values similar to those of vehicle-treated controls, whereas Zn and/or DFO treatments decreased the P:M, but not to an extent comparable to the control values (Supplementary Material, Fig. S4B; for Zn: from 230 to 196% of controls; $P = 0.03$; for DFO: from 230 to 176% of controls; $P = 0.03$; Zn + DFO: from 230 to 176%; $P = 0.05$). The treatment of PS cells with Zn or DFO partly restored the activity of Complex V (for Zn: from 45 to 66% of controls; $P = 0.007$; for DFO: from 45 to 56% of controls; $P = 0.005$), whereas the combination of iron chelation and Zn supplementation increased ATPase activity to control levels.

Lower ZnT6 protein content in PS cells

The same outcome of the parameters tested under Table 6 with zinc added to PS cells either as $ZnCl_2$ or as a zinc ionophore, zinc-pyrithione (data not shown), suggested that the defect was not located at the uptake of zinc from extracellular milieu (performed by the zinc importer proteins or ZIP) but within the intracellular milieu (intracellular flux and/or cellular efflux mediated by zinc transporters, or ZnTs). We hypothesized that a defect in the ZnT system resulted in lower zinc bioavailability in PS. To this end, we determined the gene expression of the members of the ZnT family (SLC30A) in controls and cells from premutation carriers. Ten human genes have been indentified coding for ZnT protein family members (ZnT1 through ZnT10, or SLC30A1 through SLC30A10; 41), implicated in the transport of zinc out of the cytosol, either to the extracellular space (e.g. ZnT1) or into the lumen of cytoplasmic organelles (42–44). Of the transporters examined by PCR (all except ZnT9), gene expression in control cells was found for only ZnT4, ZnT6 and ZnT3 (Supplementary Material, Fig. S5). The gene expression of ZnT4 and ZnT6 was detectable in cells from premutation patients with no significant difference in levels compared with controls. No band for ZnT3 was observed in PS and in most of PA cells (all except one), and its levels were barely detectable in control cells; thus, no inference could be made regarding any changes in its level (Table 7 and Supplementary Material, Fig. S5). Western blot analysis of the ZnT4 protein (at 43 kDa) confirmed a uniform expression for ZnT4 in all premutation cells comparable to control levels (Table 7). A single ZnT6 protein of the predicted size (51 kDa) was observed in premutation cells, significantly lower only in PS relative to controls (14% of controls; $P = 0.006$; Table 7). The discrepancy between the levels of ZnT6 mRNA and protein expression in PS fibroblasts suggested that a post-transcriptional mechanism might play a role in the specific expression of the ZnT6 protein.

Low levels of the ZnT6 protein (42% of controls) were also observed in frontal cortex samples from patients that died of FXTAS (normalized by actin, controls: 0.417 ± 0.07, PS: 0.177 ± 0.05; $P = 0.048$; Supplementary Material, Fig. S6)

validating the results obtained with dermal fibroblasts (Table 7).

DISCUSSION

In this study, we showed abnormal mitochondrial function in both CNS and non-CNS (dermal fibroblasts) tissues from patients with the neurodegenerative disorder, FXTAS. All biochemical characteristics tested point to a lower ATP production, which would particularly affect neurons because of their high (sole) dependence on OXPHOS for energy supply (45–50).

Fibroblasts from premutation carriers, independently of the presence of FXTAS symptoms, when compared with controls had lower State 3u oxygen uptake rates (PA and PS 44 and 57% of age-matched controls, respectively), lower glucose consumption via OXPHOS (35% of controls), lower Complex IV activity (PA and PS 34 and 56% of age-matched controls, respectively) and higher P:M of nDNA-encoded subunits from Complexes I, IV and V (in average 3.4-fold and 2.8-fold for PA and PS, respectively).

It is noteworthy that several of the parameters tested in the biological samples segregated with the presence of FXTAS symptoms. Fibroblasts from PS when compared with those from PA had higher *FMR1* mRNA expression (3-fold; Table 1), lower Complex V activity (38% of controls), lower aconitase activity (43% of controls), higher MPPB and AFG3l2 protein expression (133 and 154% of controls, respectively), increased frataxin gene expression (2.5-fold of controls) and lower ZnT6 protein expression (14% of controls), suggesting a segregation of outcomes with the occurrence of symptoms. Some of these characteristics were also observed in brain samples from patients that died with FXTAS symptoms: abnormal ATPB P:M and relative low levels of ZnT6 protein, suggesting a parallel between the phenotype observed in PS fibroblasts and cortex.

The significant increase in the P:M of several nDNA-encoded proteins in fibroblasts from premutation carriers and frontal cortex of PS patients appears to stem from a lower import/processing capacity of precursor proteins synthesized in the cytosol. Import/processing of nDNA-encoded proteins to mitochondria is the result of the presence of both (i) energized, polarized mitochondria and (ii) cytoplasmic and mitochondrial trans-acting components of the import/processing apparatus. The membrane potential promotes the initial translocation of the positively charged presequences of preproteins (51), and further translocation of preprotein segments requires the action of the matrix heat shock protein 70, an ATP-dependent molecular chaperone (52,53). Zn-dependent mitochondrial processing peptidase (MPP; 54), the Zn-dependent mitochondrial intermediate peptidase (MIP; 55) and the inner membrane protease (IMP; 56). MPP acts on all or part of the targeting sequence as the initial processing step, whereas MIP is specifically involved in the subsequent cleavage of proteins targeted to the mitochondrial matrix (i.e. frataxin) or inner membrane (i.e. subunits of the electron transport chain; 57), among which are ATPase subunit alpha and sub unit o, MnSOD and CCO4 (32). IMP targets proteins destined to the intermembrane space (56) and, therefore, not expected to be involved in the maturation of any of the proteins analyzed in this study.

It is likely that altered zinc bioavailability in premutation carriers (in particular PS) caused by insufficient ZnT6 protein level (Table 7) might result in a lower transport of cytoplasmic zinc into the trans-Golgi network vesicles, where it may act as the limiting step for incorporating zinc into zinc-dependent proteases. Then it is reasonable to propose that a defect on both Zn-dependent proteases, MPP and MIP, underlies the decreased level of mature mitochondrial subunits [NADH dehydrogenase (ubiquinone) Fe-S protein 1, 75 kDa (NDUFS1), NADH dehydrogenase (ubiquinone) Fe-S protein 2, 49 kDa (NADUF2), NDUFS4, Complex II 70 kDa FP, CCO4, ATPB, MnSOD and frataxin) and the accumulation of precursor polypeptides (ATPB, CCO4, NDUFS4 and frataxin) observed in fibroblasts and brain samples and fibroblasts from FXTAS patients. In support of this hypothesis, supplementation of PS cells with zinc decreased the ATPB P:M, possibly restoring the zinc-dependent activities of proteases. In addition, because the increase in the ATPase specific activity was higher than the decrease in P:M, an increase in assembly/folding of subunits into Complex V seemed to have been favored (possibly through a mechanism involving the chaperone activity of zinc-dependent AFG3l2-SPG7). Compromised processing of mitochondrial proteins, especially of ETC components, can also explain the lower OXPHOS capacity of FXTAS fibroblasts observed in this study, which can further exacerbate this energy-dependent process.

A defective zinc bioavailability may result in changes in zinc-containing proteins other than those evaluated in this study (58), which could additionally contribute to the FXTAS phenotype. In this regard, it is tempting to propose that the disrupted lamin A/C structure observed in FXTAS neural cells (59) and fibroblasts (60) could result from a defective processing of the farnesylated prelamin A by the zinc-metalloproteinase FACE1 (or STE24; 61,62), suggesting that zinc-dependent proteases other than mitochondrial ones could also be affected. In addition, cells are endowed with several zinc-dependent transcription factors (e.g. TFIIIA and Sp1; 63,64), which are affected by zinc availability (65). Zn-dependent transcription factor Sp1 interacts with the promoter of several mitochondrial proteins, such as MnSOD, ATPB, CCO4 and CYTC, among others (66–71), thus an imbalance in zinc metabolism might also affect the expression of mitochondrial proteins other than the activity of zinc-dependent proteases and chaperones, as confirmed by the reduced protein expression of MnSOD, ATPB and CCO observed in fibroblasts and brain samples from premutation carriers.

Given that frataxin, protein involved in iron metabolism, is a substrate of both MPP and MIP (27,30,31), zinc supplementation of PS fibroblasts, by restoring the activities of Zn-dependent proteases, should have increased mature frataxin in mitochondria and restored the activity of iron-containing proteins such as aconitase and Complex IV, proteins known to be deficient in frataxin-deficient cells (35). However, this treatment partly restored ATPB P:M and Complex V (iron-independent) but not Complex IV activity (Table 6). To bridge this apparent discrepancy, we reasoned

that lower MPP and MIP activities along with lower content of mature frataxin resulted in iron accumulation which could not be immediately mobilized by restoring normal levels of mature frataxin. Indeed, DFO supplementation appeared critical for the rescue of Complex IV activity (Table 6) but also for ATPB P:M. Although not apparent, accumulated iron can have a detrimental role on transport/processing of precursors by any of the following processes: (i) iron-mediated inhibition of MIP activity (72), and, as a consequence, inhibition of the processing of nDNA-encoded subunits whose final destination is the matrix and inner membrane; (ii) oxidative stress, which could result in oxidative damage and direct inactivation of mitochondrial proteins (73–75); (iii) oxidative damage of mitochondrial membrane, leading to lower membrane potential and low transport/processing activity. Oxidative inactivation of proteins has been reported in pathologies associated with increased oxidative stress caused by MnSOD deficiency (76), and in several neurodegenerative diseases including progressive supranuclear palsy (77), Friedreich's ataxia (FA; 78) and Huntington disease (79). In FXTAS, we have observed increased oxidative and nitrative stress (as judged by increased tyrosine nitration of proteins) in fibroblasts from premutation carriers (1), and increased mtDNA copy number (Supplementary Material, Table S2) and ROS production (this study) in fibroblasts of premutation carriers with clinical symptoms of FXTAS.

The lack of complete recovery of some of the outcomes in PS fibroblasts treated with DFO (or Zn + DFO) compared with vehicle-treated controls can be explained by the relatively low concentrations of DFO, and short treatment period used in this study designed to mobilize prolonged accumulated iron minimizing adverse effects potentially originated from excess metal chelation. This is the basis for the therapeutic interventions used for iron-loading diseases (such as β-thalassemia; 80,81) and neurodegenerative diseases (such as FA; 81,82) which are based on the daily use of relatively low doses of chelators over long periods (3 weeks to years; 81,83,84).

Based on this study, some overlapping biochemical mechanisms and symptoms are expected between FXTAS and other diseases with (direct or indirect) defects at the mitochondrial protein import and/or iron homestasis. (i) Defective mitochondrial protein import precludes *C. elegans* from normal development promoting defective formation of the somatic gonad (85) similar to the premature ovarian insufficiency observed in female premutation carriers (86). (ii) Loss-of-function mutations in the human Tim8p homolog DDP1 causes the neurodegenerative Mohr–Tranebjaerg syndrome (87), syndrome with defective mitochondrial import machinery that presents neurological symptoms, some of which can be observed in FXTAS such as dystonia and mental deterioration. (iii) $Spg7^{-/-}$ $Afg3l2^{Emv66/+}$ mice, bearing mutations of the genes *Spg7* and *Afg3l2* (encoding proteins belonging to the mitochondrial *m*-AAA protease) displayed an early-onset severe neurological phenotype, characterized by loss of balance, tremor and ataxia, unstable mitochondrial Complexes in affected tissues and, at late stages, neurons containing structurally abnormal mitochondria defective in cytochrome *c* oxidase-succinate dehydrogenase activity (88). In addition, deletion of AFG3 prevented the growth of yeast on non-fermentable carbon sources and abrogated the degradation of mitochondrially synthesized proteins and the assembly of cytochrome *c* oxidase and F_1F_O ATPase (89). To note, although FXTAS phenotype and biochemical findings reported in this study are similar to those of $Spg7^{-/-}$ $Afg3l2^{Emv66/+}$ mice and AFG3-deleted yeast, no decreases in protein expression of AFG3l2 and MPPB were observed. However, a deficiency in the bioavailability of zinc not accompanied by a lower protein expression might still elicit lower protease/assembly activities, resulting in a phenotype similar to that of $Spg7^{-/-}$ $Afg3l2^{Emv66/+}$ mice. (iv) Age-dependent loss of trans-synaptic zinc movement has been suggested to lead to cognitive loss in Alzheimer's disease (90). Extracellular β-amyloid is aggregated by zinc (91,92), trapping this pool of synaptic zinc (90,91) and contributing to the sequestration of this metal. As an extension, genetic ablation of ZnT6 (and/or ZnT3) and/or trapping of zinc by over-expressed *FMR1* transcript may represent a phenocopy for FXTAS symptoms (2,93). (v) Some premutation carriers (15–40%) exhibit signs of autistic behavior (94–97) suggesting some overlapping mechanisms. Besides the presence of MD in children with autism and autism spectrum disorders (ASD) (98,99), transcriptional profiles from peripheral white blood cells from children with autism with a history of developmental regression presented over-expression of 24 different zinc-finger proteins, three ZIP (ZIP6, ZIP8 and ZIP10) and two ZnT (ZnT1 and ZnT5) compared with those with an early onset of ASD (100), suggesting imbalances in zinc homestasis, and possibly iron metabolism. (vi) FA, a neurodegenerative disorder caused by the expansion of a GAA trinucleotide repeat in the first intron of the frataxin gene (*FRDA*), is characterized by lower expression of frataxin protein, lower aconitase and Complex IV activities, and accumulation of iron in mitochondria (35,101). The lower Complex IV (Table 4) and aconitase activities (43% of controls; $P = 0.05$) and the beneficial effect of DFO observed in the FXTAS fibroblasts utilized in this study were all consistent with the biochemical findings reported for patients with FA (35,102–104). Furthermore, it is interesting to note that at a phenotypic level, FA and FXTAS share some common traits: gait ataxia, loss of coordination, difficulty walking and numbness in the extremities (105,106).

Concluding remarks

This study raises three important issues: (i) MD in carriers of small CGG-repeat expansions may potentiate the appearance of phenotypes consistent with other disorders (e.g. FA's, Parkinson's disease or parkinsonism, and Alzheimer's disease) that are likely to involve MD, even when the allele size is not sufficient to produce FXTAS symptoms. (ii) Subclinical MD may also predispose such carriers to environmental stressors (e.g. nutritional status), which may in turn contribute to both the penetrance and the severity of clinical involvement in FXTAS, and finally, (iii) our data demonstrate that the appearance of FXTAS symptoms segregate with the lower activity of import/processing proteases (higher P:M) modulated by zinc and iron availability. Moreover, this study implicates impaired mitochondrial proteolysis and processing as a novel pathway in the development of FXTAS.

A better understanding of this latter issue might help us to define which carriers are most likely to develop FXTAS and to design targeted, preventative therapies.

MATERIALS AND METHODS

Chemicals and biochemicals

Ethylene diamine tetra-acetic acid (EDTA), ethylene glycol tetraacetic acid, sodium succinate, mannitol, sucrose, DFO (deferoxamine) and 4-2-hydroxyethyl-1-piperazineethanesulfonic acid (HEPES) were all purchased from Sigma (St Louis, MO, USA). Tris–HCl, glycine, sodium chloride and potassium chloride were purchased from Fisher (Pittsburg, PA, USA). Bovine serum albumin (fatty-acid free) was obtained from MP Biomedicals. All other reagents were of analytical grade.

Subject samples

All studies of post-mortem and fibroblast (biopsy) tissue samples were performed with approved protocols and informed consent in accordance with the Declaration of Helsinki (107) and the Institutional Review Boards of the University of California, Davis, or Rush University Medical Center. Clinical and molecular characteristics of the panel of cultured skin fibroblasts used in this study were presented in Table 1 and under Supplementary Material, Table S1. Samples not bolded in the Supplementary information were cultured as described in ref. (1).

Cell lines and culture conditions

Skin biopsies from individuals were performed with a 3 mm punch under local anesthesia. The biopsy was diced under sterile conditions and then plated in T25 flasks in AmnioMAX^{TM}-C100 Basal Medium (Gibco, Grand Island, NY, USA) containing 15% AmnioMAX^{TM}-C100 Supplement (Gibco) at 37°C and 5% CO_2 atmosphere. Longer term cultures of cell lines indicated in bold under Supplementary Material, Table S1 were maintained in DMEM high glucose + L-glutamine + 110 mg/ml sodium pyruvate (Gibco) supplemented with 15% fetal bovine serum (HyClone) and 1X penicillin–streptomycin (pen–strep) (100 units/ml penicillin G sodium and 100 μg/ml streptomycin; Gibco). Longer term cultures of the rest of the cell lines (not bolded) were maintained in RPMI-1640 (Gibco) supplemented with 10% fetal bovine serum (Gibco) and 1X pen–strep media (100 units/ml penicillin G sodium and 100 μg/ml streptomycin sulfate; Gibco; 1). Cells were trypsinized (0.25%) when they reached 90–95% confluence, resuspended in serum-containing media and centrifuged at 200*g* for 5 min. Following removal of supernatant, cell viability and cell counts were quantified using Trypan blue exclusion using a hemocytometer. These intact cells were used for oxygen uptake experiments. Protein extracts (for enzymatic analyses) were obtained by resuspending cell pellets at a concentration of 5×10^6 cells/ml in a hypotonic buffer (20 mM HEPES, pH 7.4) supplemented with kinase, phosphatase and proteolytic inhibitors, incubating on ice for 10–15 min, homogenizing and then freezing immediately in liquid nitrogen. Protein extracts (for western blots) were obtained by homogenizing the cells and resuspending them in radio-immunoprecipitation assay (RIPA) buffer (50 mM Tris–HCl, 150 mM NaCl, 2 mM EDTA, 0.5% CA-630 octylphenoxypolyethoxyethanol (IGEPAL), 0.1% sodium dodecyl sulfate (SDS), 0.012% deoxycholate, 0.5% Triton X-100, pH 7.4) 4 ml/mg (wet pellet weight) with protease and phosphatase inhibitors.

Brain samples

Clinical and molecular characteristics of the brain samples utilized in this study are given under Table 5 and under Supplementary Material, Table S4 essentially as described previously (1). Frozen frontal cortex from controls and PS cases was powdered in the presence of liquid N_2 and homogenized in a Dounce style homogenizer with 20 downward strokes of a tight fitting pestle in RIPA buffer (50 mM Tris–HCl, 150 mM NaCl, 2 mM EDTA, 0.5% IGEPAL, 0.1% SDS, 0.012% deoxycholate, 0.5% triton X-100, pH 7.4) with protease and phosphatase inhibitors. Homogenates were transferred to centrifuge tubes and rotated overnight at 4°C followed by centrifugation at 16 000*g* at 4°C. RIPA-soluble protein fractions were quantified with BCA Protein Assay Kit (#23225, Pierce Biotechnology, Rockford, IL, USA).

Treatment of cells with zinc and DFO

Cells (1.25×10^5) were plated in two T25 and treated for 48 h at 37°C. They were incubated with the following reagents: (i) 0.01% DMSO or vehicle only; (ii) 20 μM $ZnCl_2$; (iii) 40 nM DFO; (iv) 40 nM DFO and 20 μM $ZnCl_2$. Cells were allowed to grow for 48 h, and at the end of the incubation period, the flasks were washed three times with PBS prior to harvesting them, usually at 80–90% confluence.

Oxygen uptake

The oxygen uptake of intact cell suspensions was measured using a Clark-type O_2 electrode from Hansatech (King's Lynn, UK) at 22°C as described before (1). The respiratory control ratio (RCRu) was obtained by dividing the rate of oxygen consumption in State 3u [expressed as nmol oxygen × (min × million cells)$^{-1}$] obtained in the presence of FCCP in high glucose DMEM buffer by that of State 4 (in the presence of oligomycin) expressed with the same units. States 4 and 3 as well as RCRu are parameters defined when using isolated mitochondria. However, we will use the same nomenclature applied to the cell studies performed in this project to indicate oxygen uptake under non-phosphorylating conditions (or oligomycin-resistant oxygen uptake, State 4), phosphorylating conditions (glucose-dependent and oligomycin-sensitive oxygen uptake, State 3), maximum phosphorylating capacity (as before with FCCP, an uncoupler, or State 3u) and the ratio of State 3u/State 4 to evaluate RCRu.

Enzymatic activities

All mitochondrial enzymatic and Complex activities were described in detail in ref. (98) and Supplementary information.

mtDNA copy number

The mtDNA copy number estimated by evaluating the mtDNA/nDNA ratio was determined using qPCR essentially as described in ref. (108). The mtDNA copy number in each cell was expressed as the ratio between a mitochondrial gene (*CYTB, ND1* and *ND4*) and the single-copy nuclear PK. Other experimental details were given in ref. (98) and in the Supplementary information.

Measurement of the rate of hydrogen peroxide production

The rate of H_2O_2 production in mitochondrial preparations was followed fluorometrically using 5 U/ml horseradish peroxidase (HRP) coupled to 40 μM *p*-hydroxyphenylacetic acid oxidation (109). Succinate (10 mM), in the presence of 5 μM rotenone and 3.6 μM antimycin, were used as substrates for this assay. Mitochondrial lysate (10–100 μg/assay) was added to start the reaction. Increased fluorescence at 22°C was monitored by a Shimadzu fluorimeter. Arbitrary fluorescence units per minute for the reaction were converted to amount of H_2O_2 by comparing the values to a standard curve generated over a range of H_2O_2 concentrations. H_2O_2 generation was expressed as nmol $H_2O_2 \times (\text{min} \times 10^7 \text{ cells})^{-1}$. The addition of selective inhibitors of the respiratory chain permitted delineation of sites of mitochondrial ROS production.

Expression of selected genes in cultured cells

RNA was extracted using Qiagen's RNEasy Plus extraction kit following the manufacturer's recommendations. cDNA was generated with Qiagen's Quantitect cDNA kit according to the manufacturer's protocol, quantified using Tecan's plate reader and normalized to the weakest sample of 107 ng/μl. All other experimental details were included in the Supplementary information. The approach used to test for the expression of ZnT family members in human fibroblasts followed essentially that described by Falcon-Perez and Dell'Angelica (110) with the following modifications indicated under the Supplementary information.

Western blots

All western blot procedures were performed essentially as described before (1) with the modifications indicated in the Supplementary information (Supplementary Material, Table S5).

Statistical analyses

The number of individuals *per* group was calculated from an *a priori* G power analysis (two-tailed *t*-test, alpha = 0.05, power = (1-beta) = 0.95, and $n_1 \neq n_2$) utilizing data from RCRu and Complex IV activity. This analysis indicated that we needed four to six individuals per group. All our experiments were performed with this number of individuals except PA data on Table 7. The experiments were run in duplicate or triplicates and repeated three times in independent experiments unless noted otherwise. Data were expressed as mean ± SEM and evaluated by using the *t*-test (StatSimple v2.0.5; Nidus Technologies, Toronto, Canada) and considering $P \leq 0.05$ as statistically significant.

SUPPLEMENTARY MATERIAL

Supplementary Material is available at *HMG* online.

ACKNOWLEDGEMENTS

We wish to express our gratitude to the patients and families that participated in this study. We acknowledge the generous gift of the antibody to ZnT4 from Dr Liping Huang (University of California Davis). The authors of this study do not have any competing financial interests in relation to the work described with the exception of Dr Randi Hagerman (who has received research funding for clinical trials from Neuropharm, Roche, Johnson & Johnson, Novartis, Seaside therapeutics, Curemark and Forest pharmaceuticals and she is also a consultant to Roche and Novartis) and Dr Paul Hagerman (he is a non-paid collaborator/consultant for Asuragen and has a patent application for a method for detecting *FMR1* allele size).

Conflict of Interest statement. The funding agencies were not responsible for the design and conduct of the study; collection, management, analysis and interpretation of the data; and preparation, review or approval of this manuscript. C.G. had full access to all the data in this study and takes responsibility for the integrity of the data and the accuracy of the data analysis. D.G.-A., C.I., E.B.-K. and P.J.H. developed and provided the cell lines utilized in this study. E.N. contributed significantly to the writing of this manuscript, and E.N. and C.R.I. performed all cell cultures and biochemical studies; E.N. evaluated the effects of Zn and desferal treatments. A.O.-K. and S.W. performed all experiments related to molecular biology. C.B., E.N. and D.S. performed all western blots in the brain. E.B.-K. and R.H. recruited the subjects, performed the skin biopsies and take responsibility for the integrity of the diagnostic and socio-demographic data. The authors of this publication declare that they have no conflicting financial interest in relation to the work described.

FUNDING

This work was partially supported by funds provided by Autism Speaks Foundation (#58739, C.G.), the National Institute on Aging (AG024488, P.J.H.), the National Institutes of Health Interdisciplinary Research Consortium (IRC) grant (RL1 AG032119 and UL1 DE19583, P.J.H.; RL1 AG032115, R.H.) and the Spastic Paralysis and Allied Diseases of the Central Nervous System Research Foundation of The Illinois-Eastern Iowa District Kiwanis International (E.B.-K.).

REFERENCES

1. Ross-Inta, C., Omanska-Klusek, A., Wong, S., Barrow, C., Garcia-Arocena, D., Iwahashi, C., Berry-Kravis, E., Hagerman, R.J., Hagerman, P.J. and Giulivi, C. (2010) Evidence of mitochondrial

dysfunction in fragile X-associated tremor/ataxia syndrome. *Biochem. J.*, **429**, 545–552.
2. Berry-Kravis, E., Goetz, C.G., Leehey, M.A., Hagerman, R.J., Zhang, L., Li, L., Nguyen, D., Hall, D.A., Tartaglia, N., Cogswell, J. *et al.* (2007) Neuropathic features in fragile X premutation carriers. *Am. J. Med. Genet. A*, **143**, 19–26.
3. Hagerman, R.J., Leehey, M., Heinrichs, W., Tassone, F., Wilson, R., Hills, J., Grigsby, J., Gage, B. and Hagerman, P.J. (2001) Intention tremor, parkinsonism, and generalized brain atrophy in male carriers of fragile X. *Neurology*, **57**, 127–130.
4. Jacquemont, S., Hagerman, R.J., Leehey, M.A., Hall, D.A., Levine, R.A., Brunberg, J.A., Zhang, L., Jardini, T., Gane, L.W., Harris, S.W. *et al.* (2004) Penetrance of the fragile X-associated tremor/ataxia syndrome in a premutation carrier population. *JAMA*, **291**, 460–469.
5. Greco, C.M., Berman, R.F., Martin, R.M., Tassone, F., Schwartz, P.H., Chang, A., Trapp, B.D., Iwahashi, C., Brunberg, J., Grigsby, J. *et al.* (2006) Neuropathology of fragile X-associated tremor/ataxia syndrome (FXTAS). *Brain*, **129**, 243–255.
6. Greco, C.M., Hagerman, R.J., Tassone, F., Chudley, A.E., Del Bigio, M.R., Jacquemont, S., Leehey, M. and Hagerman, P.J. (2002) Neuronal intranuclear inclusions in a new cerebellar tremor/ataxia syndrome among fragile X carriers. *Brain*, **125**, 1760–1771.
7. Tassone, F., Hagerman, R.J., Garcia-Arocena, D., Khandjian, E.W., Greco, C.M. and Hagerman, P.J. (2004) Intranuclear inclusions in neural cells with premutation alleles in fragile X associated tremor/ataxia syndrome. *J. Med. Genet.*, **41**, e43.
8. Beckel-Mitchener, A. and Greenough, W.T. (2004) Correlates across the structural, functional, and molecular phenotypes of fragile X syndrome. *Ment. Retard. Dev. Disabil. Res. Rev.*, **10**, 53–59.
9. El-Osta, A. (2002) FMR1 silencing and the signals to chromatin: a unified model of transcriptional regulation. *Biochem. Biophys. Res. Commun.*, **295**, 575–581.
10. Oberle, I., Rousseau, F., Heitz, D., Kretz, C., Devys, D., Hanauer, A., Boue, J., Bertheas, M. and Mandel, J. (1991) Instability of a 550-base pair DNA segment and abnormal methylation in fragile X syndrome. *Science*, **252**, 1097–1102.
11. Verkerk, A.J., Pieretti, M., Sutcliffe, J.S., Fu, Y.H., Kuhl, D.P., Pizzuti, A., Reiner, O., Richards, S., Victoria, M.F., Zhang, F.P. *et al.* (1991) Identification of a gene (FMR-1) containing a CGG repeat coincident with a breakpoint cluster region exhibiting length variation in fragile X syndrome. *Cell*, **65**, 905–914.
12. Tassone, F., Hagerman, R.J., Taylor, A.K., Gane, L.W., Godfrey, T.E. and Hagerman, P.J. (2000) Elevated levels of FMR1 mRNA in carrier males: a new mechanism of involvement in the fragile-X syndrome. *Am. J. Hum. Genet.*, **66**, 6–15.
13. Tassone, F., Hagerman, R.J., Taylor, A.K., Mills, J.B., Harris, S.W., Gane, L.W. and Hagerman, P.J. (2000) Clinical involvement and protein expression in individuals with the FMR1 premutation. *Am. J. Hum. Genet.*, **91**, 144–152.
14. Kenneson, A., Zhang, F., Hagedorn, C.H. and Warren, S.T. (2001) Reduced FMRP and increased FMR1 transcription is proportionally associated with CGG repeat number in intermediate-length and premutation carriers. *Hum. Mol. Genet.*, **10**, 1449–1454.
15. Gokden, M., Al-Hinti, J.T. and Harik, S.I. (2009) Peripheral nervous system pathology in fragile X tremor/ataxia syndrome (FXTAS). *Neuropathology*, **29**, 280–284.
16. Greco, C.M., Soontrapornchai, K., Wirojanan, J., Gould, J.E., Hagerman, P.J. and Hagerman, R.J. (2007) Testicular and pituitary inclusion formation in fragile X associated tremor/ataxia syndrome. *J. Urol.*, **177**, 1434–1437.
17. Chance, B. and Williams, G.R. (1955) A simple and rapid assay of oxidative phosphorylation. *Nature*, **175**, 1120–1121.
18. Chance, B. and Williams, G.R. (1956) The respiratory chain and oxidative phosphorylation. *Adv. Enzymol. Relat. Subj. Biochem.*, **17**, 65–134.
19. Barrientos, A., Casademont, J., Cardellach, F., Estivill, X., Urbano-Marquez, A. and Nunes, V. (1997) Reduced steady-state levels of mitochondrial RNA and increased mitochondrial DNA amount in human brain with aging. *Brain Res. Mol. Brain Res.*, **52**, 284–289.
20. Lee, H.C., Yin, P.H., Lu, C.Y., Chi, C.W. and Wei, Y.H. (2000) Increase of mitochondria and mitochondrial DNA in response to oxidative stress in human cells. *Biochem. J.*, **348**, 425–432.
21. Masayesva, B.G., Mambo, E., Taylor, R.J., Goloubeva, O.G., Zhou, S., Cohen, Y., Minhas, K., Koch, W., Sciubba, J., Alberg, A.J. *et al.* (2006) Mitochondrial DNA content increase in response to cigarette smoking. *Cancer Epidemiol. Biomarkers Prev.*, **15**, 19–24.
22. May-Panloup, P., Chretien, M.F., Savagner, F., Vasseur, C., Jean, M., Malthiery, Y. and Reynier, P. (2003) Increased sperm mitochondrial DNA content in male infertility. *Hum. Reprod.*, **18**, 550–556.
23. Noack, H., Bednarek, T., Heidler, J., Ladig, R., Holtz, J. and Szibor, M. (2006) TFAM-dependent and independent dynamics of mtDNA levels in C2C12 myoblasts caused by redox stress. *Biochim. Biophys. Acta*, **1760**, 141–150.
24. Giulivi, C., Boveris, A. and Cadenas, E. (1999) In Gilbert, D. and Colton, C. (eds), *Reactive Oxygen Species in Biological Systems: An Interdisciplinary Approach*. Kluwer Academic/Plenum Publishers, New York, NY, pp. 77–102.
25. Arakane, F., Kallen, C.B., Watari, H., Foster, J.A., Sepuri, N.B., Pain, D., Stayrook, S.E., Lewis, M., Gerton, G.L. and Strauss, J.F. III (1998) The mechanism of action of steroidogenic acute regulatory protein (StAR). StAR acts on the outside of mitochondria to stimulate steroidogenesis. *J. Biol. Chem.*, **273**, 16339–16345.
26. Jaussi, R., Sonderegger, P., Fluckiger, J. and Christen, P. (1982) Biosynthesis and topogenesis of aspartate aminotransferase isoenzymes in chicken embryo fibroblasts. The precursor of the mitochondrial isoenzyme is either imported into mitochondria or degraded in the cytosol. *J. Biol. Chem.*, **257**, 13334–13340.
27. Condo, I., Ventura, N., Malisan, F., Rufini, A., Tomassini, B. and Testi, R. (2007) In vivo maturation of human frataxin. *Hum. Mol. Genet.*, **16**, 1534–1540.
28. Cavadini, P., Adamec, J., Taroni, F., Gakh, O. and Isaya, G. (2000) Two-step processing of human frataxin by mitochondrial processing peptidase. Precursor and intermediate forms are cleaved at different rates. *J. Biol. Chem.*, **275**, 41469–41475.
29. Martinelli, P., La Mattina, V., Bernacchia, A., Magnoni, R., Cerri, F., Cox, G., Quattrini, A., Casari, G. and Rugarli, E.I. (2009) Genetic interaction between the m-AAA protease isoenzymes reveals novel roles in cerebellar degeneration. *Hum. Mol. Genet.*, **18**, 2001–2013.
30. Koutnikova, H., Campuzano, V. and Koenig, M. (1998) Maturation of wild-type and mutated frataxin by the mitochondrial processing peptidase. *Hum. Mol. Genet.*, **7**, 1485–1489.
31. Gordon, D.M., Shi, Q., Dancis, A. and Pain, D. (1999) Maturation of frataxin within mammalian and yeast mitochondria: one-step processing by matrix processing peptidase. *Hum. Mol. Genet.*, **8**, 2255–2262.
32. Hendrick, J.P., Hodges, P.E. and Rosenberg, L.E. (1989) Survey of amino-terminal proteolytic cleavage sites in mitochondrial precursor proteins: leader peptides cleaved by two matrix proteases share a three-amino acid motif. *Proc. Natl Acad. Sci. USA*, **86**, 4056–4060.
33. Xu, G., Shin, S.B. and Jaffrey, S.R. (2009) Global profiling of protease cleavage sites by chemoselective labeling of protein N-termini. *Proc. Natl Acad. Sci. USA*, **106**, 19310–19315.
34. Martinelli, P. and Rugarli, E.I. (2010) Emerging roles of mitochondrial proteases in neurodegeneration. *Biochim. Biophys. Acta*, **1797**, 1–10.
35. Napoli, E., Morin, D., Bernhardt, R., Buckpitt, A. and Cortopassi, G. (2007) Hemin rescues adrenodoxin, heme a and cytochrome oxidase activity in frataxin-deficient oligodendroglioma cells. *Biochim. Biophys. Acta*, **1772**, 773–780.
36. Keberle, H. (1964) The biochemistry of deferrioxamine and its relation to iron metabolism. *Ann. N. Y. Acad. Sci.*, **119**, 758–768.
37. Ackland, M.L., Danks, D.M. and McArdle, H.J. (1988) Studies of the mechanism of zinc uptake by human fibroblasts. *J. Cell Physiol.*, **135**, 521–526.
38. Ackland, M.L., Danks, D.M. and McArdle, H.J. (1989) Zinc transport by fibroblasts from patients with acrodermatitis enteropathica. *Biol. Trace Elem. Res.*, **22**, 257–263.
39. Ackland, M.L. and McArdle, H.J. (1990) Significance of extracellular zinc-binding ligands in the uptake of zinc by human fibroblasts. *J. Cell Physiol.*, **145**, 409–413.
40. Forbes, I.J., Zalewski, P.D., Hurst, N.P., Giannakis, C. and Whitehouse, M.W. (1989) Zinc increases phorbol ester receptors in intact B-cells, neutrophil polymorphs and platelets. *FEBS Lett.*, **247**, 445–447.
41. McMahon, R.J. and Cousins, R.J. (1998) Mammalian zinc transporters. *J. Nutr.*, **128**, 667–670.
42. Devergnas, S., Chimienti, F., Naud, N., Pennequin, A., Coquerel, Y., Chantegrel, J., Favier, A. and Seve, M. (2004) Differential regulation of

zinc efflux transporters ZnT-1, ZnT-5 and ZnT-7 gene expression by zinc levels: a real-time RT-PCR study. *Biochem. Pharmacol.*, **68**, 699–709.
43. Gaither, L.A. and Eide, D.J. (2001) Eukaryotic zinc transporters and their regulation. *BioMetals*, **14**, 251–270.
44. Kelleher, S.L. and Lonnerdal, B. (2002) Zinc transporters in the rat mammary gland respond to marginal zinc and vitamin A intakes during lactation. *J. Nutr.*, **132**, 3280–3285.
45. Davey, G.P., Peuchen, S. and Clark, J.B. (1998) Energy thresholds in brain mitochondria. Potential involvement in neurodegeneration. *J. Biol. Chem.*, **273**, 12753–12757.
46. Mazzio, E.A., Reams, R.R. and Soliman, K.F. (2004) The role of oxidative stress, impaired glycolysis and mitochondrial respiratory redox failure in the cytotoxic effects of 6-hydroxydopamine in vitro. *Brain Res.*, **1004**, 29–44.
47. Fornuskova, D., Brantova, O., Tesarova, M., Stiburek, L., Honzik, T., Wenchich, L., Tietzeova, E., Hansikova, H. and Zeman, J. (2008) The impact of mitochondrial tRNA mutations on the amount of ATP synthase differs in the brain compared to other tissues. *Biochim. Biophys. Acta*, **1782**, 317–325.
48. Rossignol, R., Letellier, T., Malgat, M., Rocher, C. and Mazat, J.P. (2000) Tissue variation in the control of oxidative phosphorylation: implication for mitochondrial diseases. *Biochem. J.*, **347**, 45–53.
49. Chow, C.W. and Thorburn, D.R. (2000) Morphological correlates of mitochondrial dysfunction in children. *Hum. Reprod.*, **15**(Suppl. 2), 68–78.
50. Nissenkorn, A., Michelson, M., Ben-Zeev, B. and Lerman-Sagie, T. (2001) Inborn errors of metabolism: a cause of abnormal brain development. *Neurology*, **56**, 1265–1272.
51. Martin, J., Mahlke, K. and Pfanner, N. (1991) Role of an energized inner membrane in mitochondrial protein import. Delta psi drives the movement of presequences. *J. Biol. Chem.*, **266**, 18051–18057.
52. Kang, P.J., Ostermann, J., Shilling, J., Neupert, W., Craig, E.A. and Pfanner, N. (1990) Requirement for hsp70 in the mitochondrial matrix for translocation and folding of precursor proteins. *Nature*, **348**, 137–143.
53. Scherer, P.E., Krieg, U.C., Hwang, S.T., Vestweber, D. and Schatz, G. (1990) A precursor protein partly translocated into yeast mitochondria is bound to a 70 kd mitochondrial stress protein. *EMBO J.*, **9**, 4315–4322.
54. Luciano, P. and Geli, V. (1996) The mitochondrial processing peptidase: function and specificity. *Experientia*, **52**, 1077–1082.
55. Isaya, G., Kalousek, F. and Rosenberg, L.E. (1992) Sequence analysis of rat mitochondrial intermediate peptidase: similarity to zinc metallopeptidases and to a putative yeast homologue. *Proc. Natl Acad. Sci. USA*, **89**, 8317–8321.
56. Schneider, A., Behrens, M., Scherer, P., Pratje, E., Michaelis, G. and Schatz, G. (1991) Inner membrane protease I, an enzyme mediating intramitochondrial protein sorting in yeast. *EMBO J.*, **10**, 247–254.
57. Branda, S.S. and Isaya, G. (1995) Prediction and identification of new natural substrates of the yeast mitochondrial intermediate peptidase. *J. Biol. Chem.*, **270**, 27366–27373.
58. Udom, A.O. and Brady, F.O. (1980) Reactivation in vitro of zinc-requiring apo-enzymes by rat liver zinc-thionein. *Biochem. J.*, **187**, 329–335.
59. Arocena, D.G., Iwahashi, C.K., Won, N., Beilina, A., Ludwig, A.L., Tassone, F., Schwartz, P.H. and Hagerman, P.J. (2005) Induction of inclusion formation and disruption of lamin A/C structure by premutation CGG-repeat RNA in human cultured neural cells. *Hum. Mol. Genet.*, **14**, 3661–3671.
60. Garcia-Arocena, D., Yang, J.E., Brouwer, J.R., Tassone, F., Iwahashi, C., Berry-Kravis, E.M., Goetz, C.G., Sumis, A.M., Zhou, L., Nguyen, D.V. *et al.* (2010) Fibroblast phenotype in male carriers of FMR1 premutation alleles. *Hum. Mol. Genet.*, **19**, 299–312.
61. Corrigan, D.P., Kuszczak, D., Rusinol, A.E., Thewke, D.P., Hrycyna, C.A., Michaelis, S. and Sinensky, M.S. (2005) Prelamin A endoproteolytic processing in vitro by recombinant Zmpste24. *Biochem. J.*, **387**, 129–138.
62. Liu, B. and Zhou, Z. (2008) Lamin A/C, laminopathies and premature ageing. *Histol. Histopathol.*, **23**, 747–763.
63. Kadonaga, J.T., Carner, K.R., Masiarz, F.R. and Tjian, R. (1987) Isolation of cDNA encoding transcription factor Sp1 and functional analysis of the DNA binding domain. *Cell*, **51**, 1079–1090.
64. Moreland, R.J., Dresser, M.E., Rodgers, J.S., Roe, B.A., Conaway, J.W., Conaway, R.C. and Hanas, J.S. (2000) Identification of a transcription factor IIIA-interacting protein. *Nucleic Acids Res.*, **28**, 1986–1993.
65. Zeng, J., Vallee, B.L. and Kagi, J.H. (1991) Zinc transfer from transcription factor IIIA fingers to thionein clusters. *Proc. Natl Acad. Sci. USA*, **88**, 9984–9988.
66. Evans, M.J. and Scarpulla, R.C. (1988) Both upstream and intron sequence elements are required for elevated expression of the rat somatic cytochrome c gene in COS-1 cells. *Mol. Cell Biol.*, **8**, 35–41.
67. Carter, R.S., Bhat, N.K., Basu, A. and Avadhani, N.G. (1992) The basal promoter elements of murine cytochrome c oxidase subunit IV gene consist of tandemly duplicated ets motifs that bind to GABP-related transcription factors. *J. Biol. Chem.*, **267**, 23418–23426.
68. Basu, A., Park, K., Atchison, M.L., Carter, R.S. and Avadhani, N.G. (1993) Identification of a transcriptional initiator element in the cytochrome c oxidase subunit Vb promoter which binds to transcription factors NF-E1 (YY-1,delta) and Sp1. *J. Biol. Chem.*, **268**, 4188–4196.
69. Connor, M.K., Irrcher, I. and Hood, D.A. (2001) Contractile activity-induced transcriptional activation of cytochrome c involves Sp1 and is proportional to mitochondrial ATP synthesis in C2C12 muscle cells. *J. Biol. Chem.*, **276**, 15898–15904.
70. Zaid, A., Li, R., Luciakova, K., Barath, P., Nery, S. and Nelson, B.D. (1999) On the role of the general transcription factor Sp1 in the activation and repression of diverse mammalian oxidative phosphorylation genes. *J. Bioenerg. Biomembr.*, **31**, 129–135.
71. Ohta, S., Tomura, H., Matsuda, K. and Kagawa, Y. (1988) Gene structure of the human mitochondrial adenosine triphosphate synthase beta subunit. *J. Biol. Chem.*, **263**, 11257–11262.
72. Kalousek, F., Isaya, G. and Rosenberg, L.E. (1992) Rat liver mitochondrial intermediate peptidase (MIP): purification and initial characterization. *EMBO J.*, **11**, 2803–2809.
73. Dhanasekaran, A., Kotamraju, S., Kalivendi, S.V., Matsunaga, T., Shang, T., Keszler, A., Joseph, J. and Kalyanaraman, B. (2004) Supplementation of endothelial cells with mitochondria-targeted antioxidants inhibit peroxide-induced mitochondrial iron uptake, oxidative damage, and apoptosis. *J. Biol. Chem.*, **279**, 37575–37587.
74. Bulteau, A.L., Dancis, A., Gareil, M., Montagne, J.J., Camadro, J.M. and Lesuisse, E. (2007) Oxidative stress and protease dysfunction in the yeast model of Friedreich ataxia. *Free Rad. Biol. Med.*, **42**, 1561–1570.
75. Cantu, D., Schaack, J. and Patel, M. (2009) Oxidative inactivation of mitochondrial aconitase results in iron and H2O2-mediated neurotoxicity in rat primary mesencephalic cultures. *PLoS ONE*, **4**, e7095.
76. Williams, M.D., Van Remmen, H., Conrad, C.C., Huang, T.T., Epstein, C.J. and Richardson, A. (1998) Increased oxidative damage is correlated to altered mitochondrial function in heterozygous manganese superoxide dismutase knockout mice. *J. Biol. Chem.*, **273**, 28510–28515.
77. Park, L.C., Albers, D.S., Xu, H., Lindsay, J.G., Beal, M.F. and Gibson, G.E. (2001) Mitochondrial impairment in the cerebellum of the patients with progressive supranuclear palsy. *J. Neurosci. Res.*, **66**, 1028–1034.
78. Bradley, J.L., Blake, J.C., Chamberlain, S., Thomas, P.K., Cooper, J.M. and Schapira, A.H. (2000) Clinical, biochemical and molecular genetic correlations in Friedreich's ataxia. *Hum. Mol. Genet.*, **9**, 275–282.
79. Tabrizi, S.J., Cleeter, M.W., Xuereb, J., Taanman, J.W., Cooper, J.M. and Schapira, A.H. (1999) Biochemical abnormalities and excitotoxicity in Huntington's disease brain. *Ann. Neurol.*, **45**, 25–32.
80. Rund, D. and Rachmilewitz, E. (2005) Beta-thalassemia. *New Engl. J. Med.*, **353**, 1135–1146.
81. Brittenham, G.M. (2011) Iron-chelating therapy for transfusional iron overload. *New Engl. J. Med.*, **364**, 146–156.
82. Lim, C.K., Kalinowski, D.S. and Richardson, D.R. (2008) Protection against hydrogen peroxide-mediated cytotoxicity in Friedreich's ataxia fibroblasts using novel iron chelators of the 2-pyridylcarboxaldehyde isonicotinoyl hydrazone class. *Mol. Pharmacol.*, **74**, 225–235.
83. Kwiatkowski, J.L. (2010) Oral iron chelators. *Hematol. Oncol. Clin. North Am.*, **24**, 229–248.
84. Wong, C.S., Kwok, J.C. and Richardson, D.R. (2004) PCTH: a novel orally active chelator of the aroylhydrazone class that induces iron excretion from mice. *Biochim. Biophys. Acta*, **1739**, 70–80.
85. Curran, S.P., Leverich, E.P., Koehler, C.M. and Larsen, P.L. (2004) Defective mitochondrial protein translocation precludes normal Caenorhabditis elegans development. *J. Biol. Chem.*, **279**, 54655–54662.
86. Allingham-Hawkins, D.J., Babul-Hirji, R., Chitayat, D., Holden, J.J., Yang, K.T., Lee, C., Hudson, R., Gorwill, H., Nolin, S.L., Glicksman, A.

et al. (1999) Fragile X premutation is a significant risk factor for premature ovarian failure: the International Collaborative POF in Fragile X study—preliminary data. *Am. J. Med. Genet.*, **83**, 322–325.
87. Koehler, C.M., Leuenberger, D., Merchant, S., Renold, A., Junne, T. and Schatz, G. (1999) Human deafness dystonia syndrome is a mitochondrial disease. *Proc. Natl Acad. Sci. USA*, **96**, 2141–2146.
88. Bolot, J.F., Robert, D., Chemorin, B., Fournier, G., Thomas, L., Buffat, J. and Bertoye, A. (1977) Assisted ventilation at home by tracheotomy in subjects with chronic respiratory insufficiency. *Minerva Med.*, **68**, 409–414.
89. Frigerio, B., Ravazola, M., Ito, S., Buffa, R., Capella, C., Solcia, E. and Orci, L. (1977) Histochemical and ultrastructural identification of neurotensin cells in the dog ileum. *Histochemistry*, **54**, 123–131.
90. Adlard, P.A., Parncutt, J.M., Finkelstein, D.I. and Bush, A.I. (2010) Cognitive loss in zinc transporter-3 knock-out mice: a phenocopy for the synaptic and memory deficits of Alzheimer's disease? *J. Neurosci.*, **30**, 1631–1636.
91. Cherny, R.A., Atwood, C.S., Xilinas, M.E., Gray, D.N., Jones, W.D., McLean, C.A., Barnham, K.J., Volitakis, I., Fraser, F.W., Kim, Y.S. *et al.* (2001) Treatment with a copper-zinc chelator markedly and rapidly inhibits Œ≤-amyloid accumulation in Alzheimer's disease transgenic mice. *Neuron*, **30**, 665–676.
92. Lee, J.Y., Cole, T.B., Palmiter, R.D., Suh, S.W. and Koh, J.Y. (2002) Contribution by synaptic zinc to the gender-disparate plaque formation in human Swedish mutant APP transgenic mice. *Proc. Natl Acad. Sci. USA*, **99**, 7705–7710.
93. Bourgeois, J.A., Cogswell, J.B., Hessl, D., Zhang, L., Ono, M.Y., Tassone, F., Farzin, F., Brunberg, J.A., Grigsby, J. and Hagerman, R.J. (2007) Cognitive, anxiety and mood disorders in the fragile X-associated tremor/ataxia syndrome. *Gen. Hosp. Psychiatry*, **29**, 349–356.
94. Reiss, A.L. and Freund, L. (1990) Fragile X syndrome, DSM-III-R, and autism. *J. Am. Acad. Child. Adolesc. Psychiatry*, **29**, 885–891.
95. Feinstein, C. and Reiss, A.L. (1998) Autism: the point of view from fragile X studies. *J. Autism Dev. Disord.*, **28**, 393–405.
96. Goodlin-Jones, B.L., Tassone, F., Gane, L.W. and Hagerman, R.J. (2004) Autistic spectrum disorder and the fragile X premutation. *J. Dev. Behav. Pediatr.*, **25**, 392–398.
97. Farzin, F., Perry, H., Hessl, D., Loesch, D., Cohen, J., Bacalman, S., Gane, L., Tassone, F., Hagerman, P. and Hagerman, R. (2006) Autism spectrum disorders and attention-deficit/hyperactivity disorder in boys with the fragile X premutation. *J. Dev. Behav. Pediatr.*, **27**, S137–S144.
98. Giulivi, C., Zhang, Y.-F., Omanska-Klusek, A., Ross-Inta, C.M., Wong, S., Hertz-Picciotto, I., Tassone, F. and Pessah, I.N. (2010) Mitochondrial dysfunction in autism. *JAMA*, **304**, 2389–2396.
99. Oliveira, G., Diogo, L., Grazina, M., Garcia, P., Ataide, A., Marques, C., Miguel, T., Borges, L., Vicente, A.M. and Oliveira, C.R. (2005) Mitochondrial dysfunction in autism spectrum disorders: a population-based study. *Dev. Med. Child Neurol.*, **47**, 185–189.
100. Gregg, J.P., Lit, L., Baron, C.A., Hertz-Picciotto, I., Walker, W., Davis, R.A., Croen, L.A., Ozonoff, S., Hansen, R., Pessah, I.N. *et al.* (2008) Gene expression changes in children with autism. *Genomics*, **91**, 22–29.
101. Campuzano, V., Montermini, L., Molto, M.D., Pianese, L., Cossee, M., Cavalcanti, F., Monros, E., Rodius, F., Duclos, F., Monticelli, A. *et al.* (1996) Friedreich's ataxia: autosomal recessive disease caused by an intronic GAA triplet repeat expansion. *Science*, **271**, 1423–1427.
102. Wong, A., Yang, J., Cavadini, P., Gellera, C., Lonnerdal, B., Taroni, F. and Cortopassi, G. (1999) The Friedreich's ataxia mutation confers cellular sensitivity to oxidant stress which is rescued by chelators of iron and calcium and inhibitors of apoptosis. *Hum. Mol. Genet.*, **8**, 425–430.
103. Kontoghiorghes, G.J., Efstathiou, A., Kleanthous, M., Michaelides, Y. and Kolnagou, A. (2009) Risk/benefit assessment, advantages over other drugs and targeting methods in the use of deferiprone as a pharmaceutical antioxidant in iron loading and non iron loading conditions. *Hemoglobin*, **33**, 386–397.
104. Richardson, D.R. (2004) Novel chelators for central nervous system disorders that involve alterations in the metabolism of iron and other metal ions. *Ann. N. Y. Acad. Sci.*, **1012**, 326–341.
105. Delatycki, M.B., Williamson, R. and Forrest, S.M. (2000) Friedreich ataxia: an overview. *J. Med. Genet.*, **37**, 1–8.
106. Leehey, M.A. (2009) Fragile X-associated tremor/ataxia syndrome: clinical phenotype, diagnosis, and treatment. *J. Invest. Med.*, **57**, 830–836.
107. World Medical Association (2000) Declaration of Helsinki: ethical principles for medical research involving human subjects. *JAMA*, 284, 3043–3045.
108. Ross-Inta, C.M., Zhang, Y.F., Almendares, A. and Giulivi, C. (2009) Threonine-deficient diets induced changes in hepatic bioenergetics. *Am. J. Physiol. Gastrointest. Liver Physiol.*, **296**, G1130–G1139.
109. Sarkela, T.M., Berthiaume, J., Elfering, S., Gybina, A.A. and Giulivi, C. (2001) The modulation of oxygen radical production by nitric oxide in mitochondria. *J. Biol. Chem.*, **276**, 6945–6949.
110. Falcon-Perez, J.M. and Dell'Angelica, E.C. (2007) Zinc transporter 2 (SLC30A2) can suppress the vesicular zinc defect of adaptor protein 3-depleted fibroblasts by promoting zinc accumulation in lysosomes. *Exp. Cell Res.*, **313**, 1473–1483.